LUND UNIVERSITY

Differential Optical-absorption Spectroscopy (doas) System For Urban Atmospheric-pollution Monitoring

Edner, H; Ragnarson, P; Spannare, S; Svanberg, Sune

Link to publication

Differential optical absorption spectroscopy (DOAS) system for urban atmospheric pollution monitoring

Hans Edner, Pär Ragnarson, Stefan Spännare, and Sune Svanberg

We describe a fully computer-controlled differential optical absorption spectroscopy system for atmospheric air pollution monitoring. A receiving optical telescope can sequentially tune in to light beams from a number of distant high-pressure Xe lamp light sources to cover the area of a medium-sized city. A beam-finding servosystem and automatic gain control permit unattended long-time monitoring. Using an astronomical code, we can also search and track celestial sources. Selected wavelength regions are rapidly and repetitively swept by a monochromator to sensitively record the atmospheric absorption spectrum while avoiding the detrimental effects of atmospheric turbulence. By computer fitting to stored laboratory spectra, we can evaluate the path-averaged concentration of a number of important pollutants such as NO_2, SO_2, and O_3. A measurement of NH_3 and NO close to the UV limit is also demonstrated.

1. Introduction

With the growing awareness of the serious environment impact of industrial and automotive operations the need for the development of powerful measurement techniques for atmospheric air pollutants is increasing. Optical remote sensing techniques that use lidar (**li**ght **d**etection **a**nd **r**anging) and long-path absorption methods[1–3] are particularly advantageous because they permit large-area monitoring and avoid sample preparation difficulties characteristic of many point monitoring techniques. The differential absorption lidar (DIAL) technique, which uses powerful pulsed laser sources, permits a three-dimensional mapping of the atmospheric pollutants, while cw laser sources provide high spectral resolution and sensitivity in long-path absorption applications. Classical light sources combined with optical spectroscopy in differential optical absorption spectroscopy (DOAS) systems do not have the high performance of laser-based systems but, on the other hand, they can provide realistic, automated, and enduring measurement capabilities for multispecies monitoring, as demonstrated in this paper.

The DOAS technique was pioneered by Platt et al.[4–6] A number of species have been measured (see, e.g., Ref. 6). Our own work with the DOAS technique started in 1983, and includes the development of a specialized system for atmospheric Hg measurements[7] and spectroscopic investigations for O_3 (see Ref. 8) and NH_3 (see Ref. 9) monitoring. The possibility of measuring aromatic hydrocarbons has recently been investigated.[10] Here we describe a DOAS monitoring system that permits automated monitoring of the air mass above a medium-sized city and with some specialized research capabilities. The hardware description of the multipath atmospheric spectroscopy system is given in Subsection 2.A, while measurement routines and evaluation procedures are described in Subsections 2.B and 2.C, respectively. Atmospheric air pollution spectroscopy performed with the system and practical concentration evaluation are illustrated in Section 3 for NO_2, SO_2, NH_3, and NO. Examples of data collected with the system over a period of time are given in Section 4. Finally, the potential and limitations of the DOAS technique are discussed.

2. System Description

A. Hardware

A schematic diagram describing the DOAS system is shown in Fig. 1. The light source normally used for DOAS is a high-pressure Xe short-arc lamp. The lamp is placed at the focus of a spherical mirror to
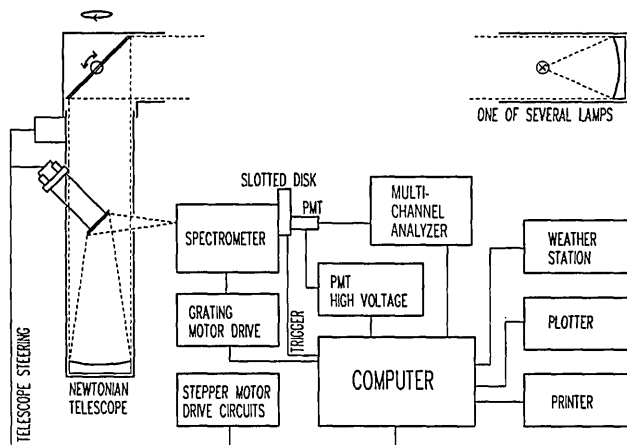
Fig. 1. Setup of the DOAS station.

obtain a well-collimated light beam. Maximum luminance is located around the cathode, and decreases towards the anode. The divergence of the beam transmitted over long distances makes it difficult to collect all light reflected by the mirror and, therefore, high maximum luminance rather than high power is required from the lamp. The Xe lamp has a broad, smooth emission spectrum except for some regions with strong emission lines in the blue and near-infrared regions. The lifetime of these lamps is of the order of six months to one year, with a tendency toward slightly more rapid intensity decay in the UV region.

The vertically positioned Newtonian receiving telescope has a primary mirror of 30-cm diameter. In front of this there is a large planar mirror, which can be rotated horizontally and vertically by stepping motors (0.47 and 0.63 mrad/step, respectively), enabling the telescope to look in different directions. To improve the angular resolution of the telescope orientation the secondary mirror is controlled by stepping motors. This unit has a resolution of 0.025 mrad/step. The dispersive instrument is a Spex 500 M spectrometer ($f/4$) with a 1200-groove/mm grating with blaze at 300 nm. A slotted disk scans the spectrum in 10 ms. The disk has 20 slits 100 μm wide and rotates at 5 revolutions/s. A mask in the focal plane limits the scan to cover approximately 40 nm. A trigger signal, generated when the slit passes an IR light barrier close to the edge of the mask, is used to synchronize the wavelength scale of each individual scan. The entrance slit of the spectrometer is normally 100 μm wide, which gives an optimum spectral resolution of 0.23 nm. The detector is an EMI 9558 QA photomultiplier tube (PMT) with a 5-cm-diameter photocathode to capture the light passing the scanning exit slit. After amplification the signal is stored in a custom-made (MCA) multichannel analyzer plug-in card in an IBM-compatible AT computer. The MCA is equipped with a 12-bit analog-to-digital converter (ADC), which divides each scan into 1024 channels and can add as many as 60,000 scans before the result is transferred to the computer.

Currently the system is arranged with three measurement paths overlooking the city of Lund, Sweden (population 50,000). Three individual Xe lamps, A, B, and C, are placed 2000, 1600, and 400 m respectively, from the receiver, as shown in Fig. 2. The optimum path length varies for different species. A trade-off has to be made between higher sensitivity for longer paths and higher transmission for shorter paths, which are less likely to be blocked by fog. The light paths are located at a height of 10 to 30 m above the ground. The diameters of the lamp telescope mirrors are 30, 15, and 30 cm, and the lamps have output powers of 500, 75, and 150 W. Normally, the lamp telescopes are sealed from the atmosphere by a quartz window for protection.

B. Measurement Routines

In a measurement sequence the telescope is first turned to the specified light source and the grating is set for the appropriate wavelength region for the first species to be measured. The voltage of the PMT tube is set to an empirical value, depending on the distance to the light source as well as its spectral power, the transmission efficiency of the atmosphere, and the spectroscopic equipment in this wavelength region. Because of thermal effects and backlash in the stepping motor machinery, the viewing direction of the telescope is optimized by adjusting the secondary mirror with stepping motors. The PMT voltage is then regulated in such a way that the signal from the interesting part of the spectrum corresponds to ~ 75% of the maximum level for the ADC. After each measurement meteorological data (wind velocity and direction) from a small weather station are measured and stored. While the MCA card is accumulating scans, the computer is free to evaluate the previous measurement, print the results, and store them in the computer on floppy disks. The results and all relevant data are stored in files in a format suitable for use in graphic presentation programs. After the measurement of a particular wavelength region is completed, a new region can be chosen for the study of different pollutants. Other light sources can then be selected.

Several celestial objects can be searched and tracked by using an astronomical code for steering the telescope.[11,12] The use of the sun, moon, and scattered sky light, together with fixed light sources, permit measurements of both the tropospheric and stratospheric concentrations of many species,[13-16] but this option is not demonstrated here.

C. Evaluation

After a light source has been selected and data acquisition has been performed according to Subsection 2.B, the atmospheric spectrum is evaluated according to the algorithms described by Platt and Perner.[6] The routine starts by subtracting the background from the recorded spectrum. The trigger signal starts the measurement before the exit slit enters the unmasked area and continues to measure a
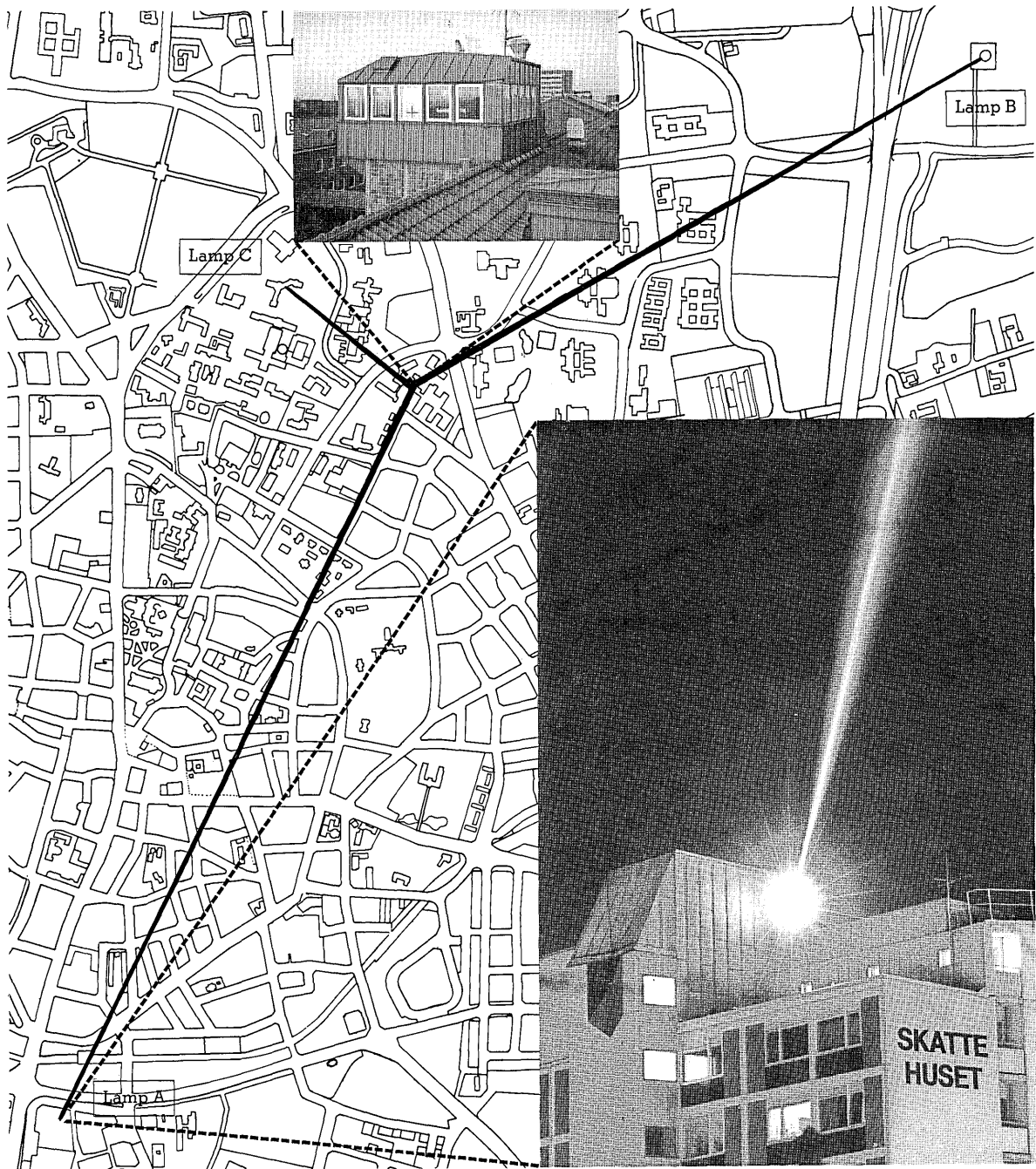
Fig. 2. Measurement paths overlooking Lund, Sweden. In the insets, photographs of the receiving station and the lamp transmitters are shown.

short while after the slit is masked again. An average of these parts of the scan is considered to be the background that is due mainly to PMT dark current and offset in the preamplifier. A portion of the spectrum is selected, and a polynomial of degree 5 or 6 is calculated to fit this part of the spectrum. The atmospheric spectrum is then divided by the polynomial and normalized. The result is a high-pass filtering that enhances the differential structure and eliminates many instrument-specific features, such as the broad structure in the lamp spectrum, as well as differences in the spectroscopic transmission and

detector sensitivity. Since the evaluation relies on the Beer–Lambert law, a logarithmic transformation of the normalized spectrum is made. The mean concentration of the species in the light path is then evaluated by correlation with as many as six different reference spectra recorded in the laboratory. Naturally the reference spectra must be recorded in the same way as the atmospheric spectrum, using the same width of the entrance slit, etc., and evaluated with the same parameters. The standard deviation of the difference between the atmospheric spectrum and the correlation spectra indicates the accuracy of

the measurement. Because of temperature effects and backlash in the spectrometer grating drive, the atmospheric spectrum may be offset a few channels with respect to the laboratory spectrum, and the correlation routine, therefore, optimizes the correlation by shifting the atmospheric spectrum within ±20 channels. The offset value and the correlation coefficient are printed and stored and can be used as an indication of the correctness of the correlated values. The integrated intensity value of the raw spectrum is also printed and stored and this indicates whether the measurement has been performed under suitable conditions. A routine of rejecting data from measurements during low-light-level conditions can be implemented. All details of the evaluation are set in an evaluation sequence menu and an evaluation parameter menu that can be stored in the computer. In this way, we have created a directory of predefined measurement cycles.

3. Atmospheric Air Pollution Spectroscopy

In Fig. 3 the evaluation of a spectrum, according to the routines described in Subsection 2.C, is shown. Figure 3(a) shows a raw spectrum obtained by adding 30,000 scans made over 5 min. The sharp edges at both ends of the spectrum are due to the masking procedure described above. In Fig. 3(a) some sharp features from the Xe lamp are evident in the spectrum. NO_2 has the strongest absorption bands in a region where the Xe lamp has strong emission lines. The relative intensity in these lamp structures is time dependent because of the aging of the lamp, so the region of evaluation that is free from these features must be chosen. This region, marked in Fig. 3(a), is shown in Fig. 3(b) together with the fitted polynomial. The differential structure is enhanced by normalization to the polynomial (dotted curve), and the final result after logarithmic transformation is shown in Fig. 3(c) together with the reference spectrum (dotted curve) to give the best fit; 15.2-μg/m^3 NO_2 over the 2000-m atmospheric path. Figure 3(d) shows the residual spectrum when the reference spectrum has been subtracted from the atmospheric spectrum. The larger structures in the residual spectrum might be related to other species present in the atmosphere or due to artifacts from the normalization to the polynomial fit. The noise in the spectrum indicates a minimum detectable absorption of 5×10^{-4} for the system, which, for the 2-km path, results in a detection limit of ~0.4 μg/m^3.

Figure 4 shows an example of a multispecies measurement at short UV wavelengths. An additional measurement path of 350-m was used, and the receiving telescope was optimized for the short UV region. In Fig. 4(a) the atmospheric spectrum (solid curve) is shown together with a reference spectrum of SO_2 scaled to represent 5.0 μg/m^3 over the 350-m path (dotted curve). The atmospheric spectrum after subtraction of the SO_2 reference spectrum is shown in Fig. 4(b) together with an NH_3 reference spectrum of 0.7 μg/m^3. The residual after subtraction of the
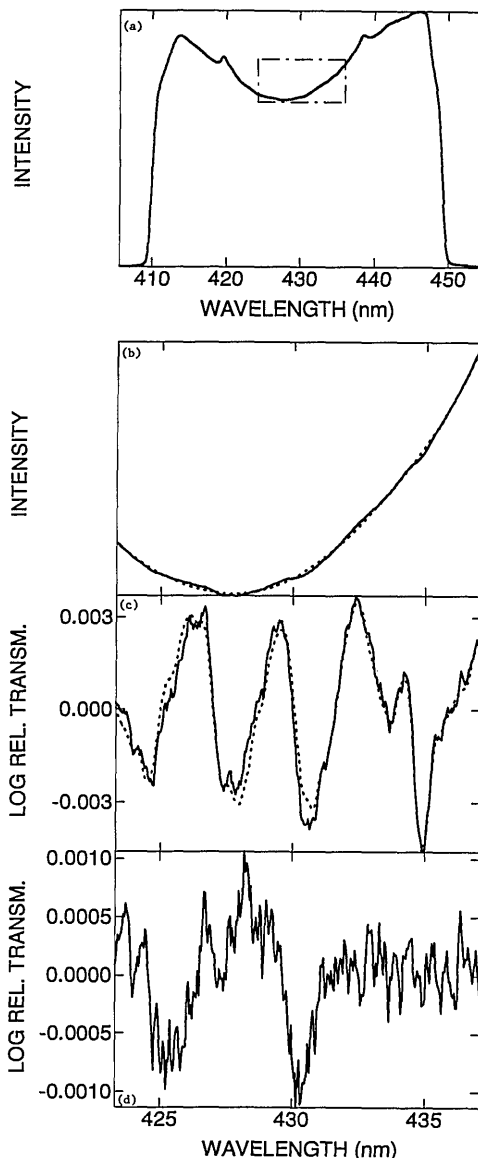

Fig. 3. Measurement of NO_2 over a 2000-m path length: (a) raw spectrum, (b) raw spectrum (solid curve) and polynomial fit (dotted curve), (c) differential spectrum (solid curve) and reference spectrum of 15.2-μg/m^3 NO_2 (dotted curve), (d) residual spectrum.

NH_3 reference is shown in Fig. 4(c) together with the reference spectrum of NO scaled to equal 2.8 μg/m^3. The final residual is shown in Fig. 4(d). As in the measurement presented in Fig. 3, the larger structures might be the result of the evaluation procedure. The noise in this measurement is, of course, greater because of the smaller light flux in this wavelength region. Multispecies spectra are normally evaluated with a simultaneous correlation of the reference spectra, as described in Subsection 2.C. Figure 4 shows the contribution from the separate species, and a sequential evaluation can be used if the correlation between the different reference spectra is small.

4. Examples of Results

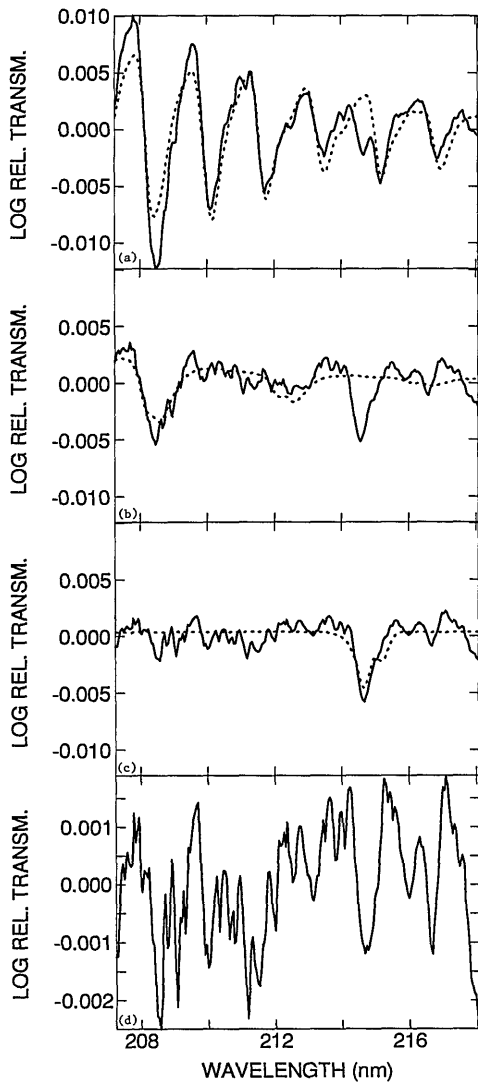Data for NO_2 in three directions recorded over 24 h are shown in Fig. 5. The influence of the morning

Fig. 4. Measurement at short UV wavelengths (350-m path length): (a) atmospheric spectrum (solid curve) and reference spectrum of 5.0-μg/m^3 SO$_2$ (dotted curve), (b) atmospheric spectrum after SO$_2$ subtraction (solid curve) and reference spectrum of 0.7-μg/m^3 NH$_3$ (dotted curve), (c) atmospheric spectrum after SO$_2$ and NH$_3$ subtraction (solid curve) and reference spectrum of 2.8-μg/m^3 NO (dotted curve), (d) residual spectrum.
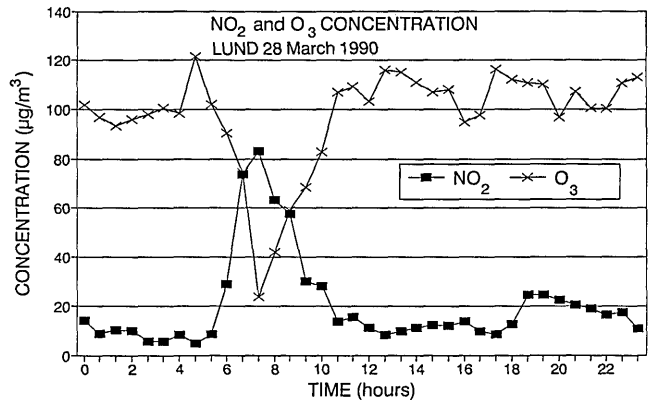

Fig. 6. NO$_2$ and O$_3$ correlations measured over 24 h (400-m path in Fig. 2).

traffic can be clearly seen. Figure 6 shows the concentration of O$_3$ and NO$_2$ for one day. In the morning the NO$_2$ concentration increases strongly because of traffic. The anticorrelation of the O$_3$ and NO$_2$ concentrations due to atmospheric chemistry is clearly seen. NO$_2$ data for one week are shown in Fig. 7. Diurnal variations related to traffic are seen. It should be noted that the period covers the Easter holidays, 1990, with 13 April (Friday) being the first free day and 17 April (Tuesday) being, again, a regular working day. Figure 8 shows the average concentration of SO$_2$ as a function of wind direction, measured between 29 May and 14 July 1990. The impact of winds from the south and southeast is clearly indicated.

5. Discussion

Detection techniques based on optical spectroscopy have many advantages compared with conventional wet chemistry instrumentation. Primarily, a mean value over a long distance is often more representative than a value from a point monitor. A large area can be monitored from one station, as shown in this study. Optical instruments can often provide rapid measurements that give values with high temporal resolution. A further advantage is the low frequency of calibration necessary. Spectroscopic instruments are also easy to computerize and DOAS
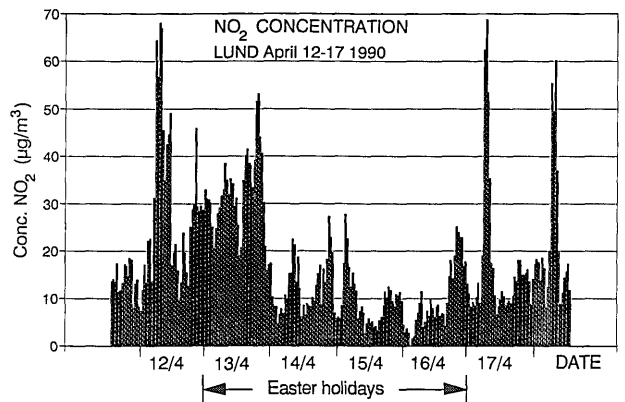

Fig. 5. NO$_2$ data during 24 h for the three directions in Fig. 2.
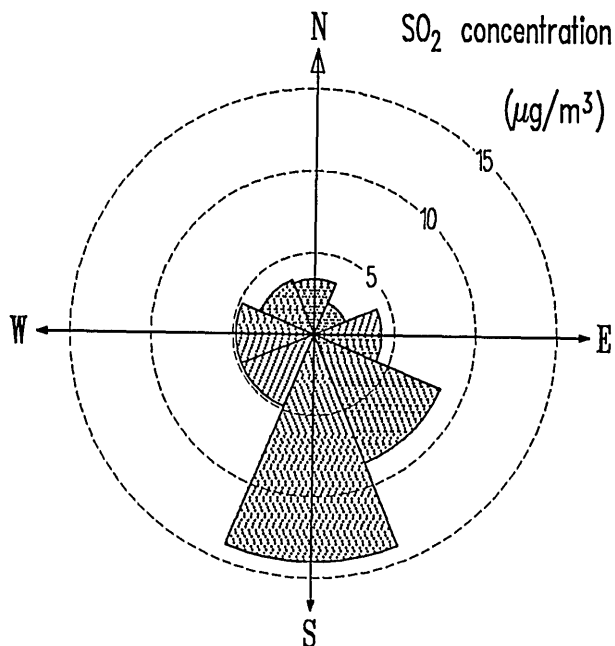

Fig. 7. NO$_2$ data for one week (2000-m path in Fig. 2).

Fig. 8. Average SO_2 concentrations as a function of the wind direction, 29 May to 14 July 1990 (2000-m path).

systems can run unattended for long periods, communicating with the operator through a modem on the telephone network for automated data reports or reprogramming. An alternative approach to the one described here is to replace the lamp telescopes with retroreflectors and to construct the transmitting lamp and receiving telescope as one unit.[17] The practical and economical benefits of replacing active lamp telescopes with passive retroreflectors encourage the use of a larger number of retroreflectors, which would ensure optimum path lengths for all meteorological conditions. Rain does normally not affect the measurements if the windows are shielded, but fog can block the light if the path is long. Haze can occasionally scatter sunlight into the receiving telescope but this effect can be compensated for in the retroreflector concept; the lamp is blocked while the scattered sunlight is measured and this signal can then be subtracted from the measurements. The atmospheric turbulence makes it necessary to measure all wavelengths simultaneously or to freeze the atmosphere by measuring the spectrum quickly enough.[18] The first approach is implemented with photodiode or CCD arrays, and has the big advantage of good light economy. Disadvantages are the sensitivity variations between different pixels and also within each pixel. These variations can change in time, and frequent calibration is, therefore, often necessary. Array detectors can also suffer from étalon effects originating from surface coatings and from substantial readout noise. To reduce detector noise, array detectors are normally cooled and therefore flushed with dry air. All this could, in principle, be handled, and these devices are used in many scientific instruments.[19,20] Historically, array detectors have been expensive, delicate, and not appropriate for

unattended long-time measurements; then the slotted disk was developed to tackle the turbulence problem the other way. Here the exit slit in the spectrometer has been replaced by a rotating slotted disk. The disadvantage of this concept is the poor light economy and the fact that the exit slit is vertical in only the middle of the scan. The spectral resolution then varies along the spectrum, in our case from 0.23 nm in the middle of the spectrum to 0.53 nm at both ends. This also means that the spectral resolution changes with a vertical translation of the spectrum in the focal plane. The practical advantages with rapid scanning devices still make them competitive in the development of new systems.[21,22]

References

1. D. K Killinger and A. Mooradian, eds. *Optical and Laser Remote Sensing Techniques* (Springer Verlag, Heidelberg, 1983).
2. K. M. Measures, *Laser Remote Sensing* (Wiley-Interscience, New York, 1984).
3. S. Svanberg "Optical Environmental Monitoring," in *Applied Laser Spectroscopy*, M. Inguscio and W. Demtröder, eds. (Plenum, New York, 1990), pp. 417–434.
4. U. Platt, D. Perner, and H. W. Pätz, "Simultaneous measurements of atmospheric CH_2O, O_3, and NO_2 by differential optical absorption," J. Geophys. Res. **84**, 6329–6335 (1979).
5. U. Platt and D. Perner, "Direct measurement of atmospheric CH_2O, HNO_2, O_3, and SO_2 by differential absorption in the near UV," J. Geophys. Res. **85**, 7453–7458 (1980).
6. U. Platt and D. Perner, "Measurements of atmospheric trace gases by long path differential UV/visible absorption spectroscopy," in *Optical and Laser Remote Sensing Techniques*, D. K. Killinger and A. Mooradian, eds. (Springer-Verlag, Heidelberg, 1983), pp. 97–105.
7. H. Edner, A. Sunesson, S. Svanberg, L. Unéus, and S. Wallin, "Differential optical absorption spectroscopy system for atmospheric mercury monitoring," Appl. Opt. **25**, 403–409 (1986).
8. H. Axelsson, H. Edner, B. Galle, P. Ragnarson, and M. Rudin, "Differential optical spectroscopy (DOAS) measurements of ozone in the 280–290 nm wavelength region," Appl. Spectrosc. **44**, 1654–1658 (1990).
9. H. Edner, R. Amer, P. Ragnarson, M. Rudin, and S. Svanberg, "Atmospheric NH_3 monitoring by long-path UV absorption spectroscopy," in *Environment and Pollution Measurement Sensors and Systems*, H. O. Nielsen, ed., Proc. Soc. Photo-Opt. Instrum. Eng. **1269**, 14–20 (1990).
10. H. Axelsson, H. Edner, A. Eilard, A. Emanuelsson, B. Galle, H. Kloo, and P. Ragnarson, "Measurements of aromatic hydrocarbons with the DOAS technique," Appl. Spectrosc. (to be published).
11. P. Duffet-Smith, *Practical Astronomy with Your Calculator*, 3rd ed. (Cambridge U. Press, Cambridge, 1988).
12. H. Karttunen, P. Kröger, H. Oja, M. Poutanen, and K. J. Donner, *Fundamental Astronomy* (Springer-Verlag, Heidelberg, 1987).

13. J. F. Noxon, "Tropospheric NO_2," J. Geophys. Res. **83**, 3051–3057 (1978).

14. J. F. Noxon, E. C. Whipple, Jr., and R. S. Hyde, "Stratospheric NO_2, 1, Observational method and behavior at mid-latitude," J. Geophys. Res. **84**, 5047–5065 (1979).

15. S. Solomon, A. L. Schmeltekopf, and R. W. Sanders, "On the interpretation of zenith sky absorption measurements," J. Geophys. Res. **92**, 8311–8319 (1987).

16. J. P. Pommereau and F. Goutail, "O_3 and NO_2 ground-based measurements by visible spectrometry during arctic winter and spring 1988," Geophys. Res. Lett. **15**, 891–894 (1988).

17. B. Galle, H. Axelsson, K. Gustavsson, P. Ragnarson, and M. Rudin, "A transmitting/receiving telescope for DOAS measurements using retroreflector techniques," submitted to Appl. Opt.

18. N. Menyuk and D. K. Killinger, "Temporal correlation measurements of pulsed dual CO_2 lidar returns," Opt. Lett. **6**, 301–303 (1981).

19. A. Wahner, R. O. Jakoubek, G. H. Mount, A. R. Ravishankara, and L. Schmeltekopf, "Remote sensing observations of daytime column NO_2 during the airborne Antarctic ozone experiment, August 22 to October 2, 1987," J. Geophys. Res. **94**, 16,619–16,632 (1989).

20. S. E. McLaren and D. H. Stedman, "Flux measurements using simultaneous long path ultraviolet and infrared spectroscopy," in *Proceedings of the Eighty-Third Air and Waste Management Association Annual Meeting* (Air and Waste Management Association, Pittsburgh, Pa., 1990), paper 90-86.6.

21. H. W. Biermann and A. M. Winer, "Recent improvements in the design and operation of a differential optical absorption spectrometer for *in situ* measurement of gaseous air pollutant," in *Proceedings of the Eighty-Third Air and Waste Management Association Annual Meeting* (Air and Waste Management Association, Pittsburgh, Pa., 1990), paper 90-87.2.

22. A. M. Winer and H. W. Biermann, "Measurements of nitrate radicals, formaldehyde, and nitrogen dioxide for the Southern California Air Quality Study by differential optical absorption spectroscopy," in *Measurement of Atmospheric Gases*, H. I. Schiff, ed., Proc. Soc. Photo-Opt. Instrum. Eng. **1433** (to be published).